J. Membrane Biol. 158, 127–136 (1997)

The Journal of
Membrane
Biology



# Regulatory Volume Decrease by SV40-transformed Rabbit Corneal Epithelial Cells Requires Ryanodine-sensitive $Ca^{2+}$-induced $Ca^{2+}$ Release

**X. Wu[1], H. Yang[1], P. Iserovich[3], J. Fischbarg[2,3], P.S. Reinach[1]**

[1]Department of Biological Sciences, State University of New York, College of Optometry, New York, NY 10010, USA
[2]Departments of Physiology and Cellular Biophysics, Columbia University, College of Physicians and Surgeons, New York, NY 10032, USA
[3]Department of Ophthalmology, Columbia University, College of Physicians and Surgeons, New York, NY 10032, USA

Received: 7 November 1996/Revised: 6 January 1997

**Abstract.** The relationship between relative cell volume and time-dependent changes in intracellular $Ca^{2+}$ concentration ($[Ca^{2+}]_i$) during exposure to hypotonicity was characterized in SV-40 transformed rabbit corneal epithelial cells (tRCE) (i). Light scattering measurements revealed rapid initial swelling with subsequent 97% recovery of relative cell volume (characteristic time ($\tau_{vr}$) was 5.9 min); (ii). Fura2-fluorescence single-cell imaging showed that $[Ca^{2+}]_i$ initially rose by 216% in 30 sec with subsequent return to near baseline level after another 100 sec. Both relative cell volume recovery and $[Ca^{2+}]_i$ transients were inhibited by either: (a) $Ca^{2+}$-free medium; (b) 5 mM $Ni^{2+}$ (inhibitor of plasmalemma $Ca^{2+}$ influx); (c) 10 μM cyclopiazonic acid, CPA (which causes depletion of intracellular $Ca^{2+}$ content); or (d) 100 μM ryanodine (inhibitor of $Ca^{2+}$ release from intracellular stores). To determine the temporal relationship between an increased plasmalemma $Ca^{2+}$ influx and the emptying of intracellular $Ca^{2+}$ stores during the $[Ca^{2+}]_i$ transients, $Mn^{2+}$ quenching of fura2-fluorescence was quantified. In the presence of CPA, hypotonic challenge increased plasmalemma $Mn^{2+}$ permeability 6-fold. However, $Mn^{2+}$ permeability remained unchanged during exposure to either: 1.100 μM ryanodine; 2.10 μM CPA and 100 μM ryanodine. This report for the first time documents the time dependence of the components of the $[Ca^{2+}]_i$ transient required for a regulatory volume decrease (RVD). The results show that ryanodine sensitive $Ca^{2+}$ release from an intracellular store leads to a subsequent increase in plasmalemma $Ca^{2+}$ influx, and that both are required for cells to undergo RVD.

*Correspondence to:* P.S. Reinach

**Key words:** Ryanodine — Volume regulation — Calcium — Capacitative $Ca^{2+}$ influx — Cornea

## Introduction

The corneal epithelium forms a permeability barrier which protects the eyes from noxious agents and infection (Klyce & Beuerman, 1988). Furthermore, it transports electrolytes from the underlying stroma to the tears, and generates a small water flow in the same direction (Klyce, 1977; Candia & Zamudio, 1995). This flow coupled with the fluid flux across the endothelium into the anterior chamber offset stromal fluid imbibition and possible loss of transparency (Fischbarg, Lim & Bourguet, 1977; Maurice, 1972). Given its location, this epithelium is subject to anisosmotic challenge. For example, during waking hours, mammalian tears are slightly hypertonic due to evaporation, whereas swimming in fresh water exposes the epithelium to hypotonicity. There is limited evidence that these cells respond by regulating their volume subsequent to swelling but not much is known about the responsible mechanisms (Wolosin & Candia, 1989). We have undertaken a characterization of epithelial volume regulatory processes by studying regulatory volume decrease (RVD) in SV40-transformed rabbit corneal epithelial cells (tRCE).

There are numerous examples of cell types which elicit RVD subsequent to a rapid transient increase in $[Ca^{2+}]_i$ (e.g., for reviews *see* Foskett, 1994; Chamberlin & Strange, 1989). The intracellular signal linking swelling to an increase in $[Ca^{2+}]_i$ can have several origins. In human platelets, release from intracellular stores (ICS) is followed by either: (a) activation of a pertussis toxin (PTX) sensitive G-protein, or (b) stimulation by arachi-

donic acid release (Margalit, et al., 1993). In cardiomyocytes, the mechanism for such $Ca^{2+}$ release was further defined; physical stretch induced increases in inositol 1,4,5 triphosphate ($IP_3$) and tetrakisphosphate accumulation, accompanying RVD (Dassouli et al., 1993). In COS 7 cells, hypotonicity also induced through the stimulation of a PTX sensitive G-protein increased hydrolysis of $IP_3$ which was associated with a transient elevation of $[Ca^{2+}]_i$ and an increase in Cl-conductance. This $[Ca^{2+}]_i$ transient solely resulted from the release of $Ca^{2+}$ from ICS (Ishii, Hashimoto & Ohmori, 1996). A second possible release pathway exists in embryonic rat aorta Ar5 cells. Release through this pathway is a result of stimulation of osmosensors located in the ICS and occurs in the absence of intracellular mediators. It can only be inhibited by a number of divalent cations (Missiaen et al., 1996).

The triggering of RVD by an increase in intracellular $Ca^{2+}$ could be a consequence of either an increase in $Ca^{2+}$ influx or could involve an initial increase in $IP_3$ receptor mediated release of $Ca^{2+}$ from ICS. Plasmalemma $Ca^{2+}$ influx can be sufficient to trigger an RVD response in different kidney cell preparations (McCarty & O'Neil, 1991*a*,*b*; Rafizadeh-Montrose & Guggino, 1991). Alternatively, efflux could involve $IP_3$-mediated release and/or release from a ryanodine sensitive pathway followed by stimulation of plasmalemma $Ca^{2+}$ influx (CICR) (Putney, 1986). In parotid gland acinar cells, CICR could be regulated by protein phosphorylation. In these cells, two different protein phosphatases attenuated carbachol stimulated $Ca^{2+}$ entry (Sakai & Ambudkar, 1996). This effect of carbachol is mediated through an increase in $IP_3$ formation which initially triggers $Ca^{2+}$ release from ICS. CICR was described in inner medullary collecting duct cells where hypotonicity elicited increases in $[Ca^{2+}]_i$ which were due to release of $Ca^{2+}$ from ICS followed by increased $Ca^{2+}$ influx across the plasma membrane (Tinel, Wehner & Sauer, 1994). In that study, either caffeine or TMB-8 were used with the assumption that they inhibit ICS $Ca^{2+}$ release. However, in some other cell types a particular concentration of caffeine may instead stimulate ICS $Ca^{2+}$ release whereas in others it may stimulate ATP dependent $Ca^{2+}$ uptake into ICS without at all affecting ICS $Ca^{2+}$ release (Walz et al., 1995; Mekhail-Ishak, Lavoie & Sharkawi, 1987). Similarly, TMB-8 can have diverse modes of action (Islam et al., 1995; Bencherif et al., 1995). However, the selectivity of ryanodine is well established as a modulator of $Ca^{2+}$ release through ICS ryanodine sensitive channels (Meissner, 1986). In human intestinal 407 cells, ryanodine selectively inhibited $Ca^{2+}$ release and RVD but the relationship between the components of the $[Ca^{2+}]_i$ transient, plasmalemma $Ca^{2+}$ influx and RVD were not resolved (Hazama & Okada, 1990). Hence, at present, although there are indications of CICR involvement in RVD, there are no reports showing that CICR is actually required for RVD. There is some indication that ryanodine-sensitive $Ca^{2+}$ release and CICR may have physiological relevance for corneal epithelial cells (Socci et al., 1993). However, the linkage of these mechanisms to a physiological response has yet to be described.

We show here that: (i) tRCE cells undergo a RVD response in response to hyposmolality; (ii) $Ca^{2+}$ signaling mediates this response; (iii) the $Ca^{2+}$ signaling pathways include stimulation of ryanodine sensitive $Ca^{2+}$ release from ICS followed by an increase in $Ca^{2+}$ influx through plasmalemma nonselective nonvoltage gated ionic pathways. Therefore, our evidence demonstrates definitively that in these cells CICR is an essential component of the cell-signaling system that mediates RVD.

## Methods and Materials

SV40-transformed rabbit corneal epithelial cells were a generous gift from Dr. Araki-Sasaki (Kinki University, Hyogo, Japan). They were cultured in DMEM/F12 as described (Araki-Sasaki, Ohashi & Sasabe, 1993).

### Determinations of $[Ca^{2+}]_i$

Cells were subcultured for two days on 22 mm diameter coverslips (12-545-01 Fisher Scientific, Pittsburgh, PA) and mounted in a thermally regulated holder (T = 37°C) placed on the stage of an inverted microscope (Nikon Diaphot 200). The volume of the chamber was 1 ml and complete solution exchange occurred in about 10 sec. The cells were illuminated with alternating 340 and 380 nm light (narrow bandpass filters ± 15 nm Filter Set 7100 Chroma Technology, Brattleboro, VT) and visualized with a Nikon 40× phase/fluor oil objective (NA = 1.3). The emitted light passed through a narrow band pass 510 nm filter (±40 nm) prior to acquisition by a digital CCD camera (≠1400, Xillix microimager, Vancouver, British Columbia). A SUN SPARC-5 workstation and Inovision® (Durham, NC) image software were used to record and analyze the fluorescence ratio (340/380 nm). Ratio images were calculated based on 10 to 20 exposures of 20–200 msec duration. They were collected every 5 sec and their mean values were converted to $[Ca^{2+}]_i$ levels with a calibration curve obtained from measurements of the $Ca^{2+}$ dependent fluorescence of fura 2-in solution. In a given microscopic field, individual cells were chosen for monitoring $[Ca^{2+}]_i$ only if they had a comparatively large cytoplasmic/nuclear ratio and homogeneous brightness.

### Determination of $[Mn^{2+}]_i$

An index of $Ca^{2+}$ influx was obtained from measurements of fura2-fluorescence quenching by $Mn^{2+}$ (Hallam, Jacob & Merritt, 1989; Jacob, 1990). Fura2-fluorescence ([fura2] = 0.5 μM) was excited at its isosbestic point (360 nm) and emission was monitored at 510 nm. The extent of fura2-fluorescence quenching by $Mn^{2+}$ (0.1–0.5 μM in Dulbecco's phosphate buffered saline, Atlanta Biologicals) was determined with a Beckman spectrofluorometer. In this range, there is a linear relationship between the quenching ($\phi$–$\phi_O$) and the $[Mn^{2+}]$ which was used to determine the rate of $Mn_i^{2+}$ accumulation and plasmalemma $Mn^{2+}$ permeability (*see Results*).

Measurements of fura2 quenching were performed as above. The

amount of initial quench measured during a linear phase lasting 35 sec was used to calculate $Mn^{2+}$ influx and plasmalemma $Mn^{2+}$ permeability. These calculations employed a modified form of the Goldman Hodgkin Katz equation and assumed an average cell height of 15 μ as well as an intracellular voltage of −70 mV.

### Determination of Cell Volume

The procedure was as described (Fischbarg et al., 1993) and is only summarized here. Cells were subcultured on 11 × 22 mm rectangular glass coverslips until they reached 70–80% confluency (usually two days). They were secured in a cylindrical glass shell vial using a Teflon cap fitted with stainless steel perfusion inlet and outlet ports, a slot for mounting a coverslip, and a steel alignment rod radiating outward from the slot for precise orientation of the coverslip. Coverslips were secured into the slot using a small compression screw. The cuvette perfusion system was thermally regulated at between 36 and 38°C, and the perfusion lines were maintained at 41°C, so that solutions being exchanged reached the chamber at the proper temperature. For solution exchanges, the superfusion rate was 15–20 ml/min. Complete vial solution exchange required about 10 sec. The suspended coverslips were illuminated with an 8-mm diameter spot of light obtained through an expander from a 5-mW helium-neon laser (model 05-LHP-151; Melles Griot, Irvine, CA). Low-angle forward scattered light was detected with a photomultiplier tube (R928, Hamamatsu, Bridgewater, NJ). The PMT was operated at around 300 V and its current output was converted to a voltage signal by a preamplifier, low-pass filtered and fed to a computer via an analog-to-digital conversion board (Labmaster, Scientific Solutions, Solon, OH) sampled at 1 Hz. The same signal went also to a strip-chart recorder; for convenience, the signal was inverted, so that cell swelling elicited an upward deflection (decreased light scattering), whereas shrinkage had an opposite effect.

### *Light Scattering Analysis*

The intensity of light scattering represented by the PMT voltage readings was converted to relative cell volume (Fischbarg et al., 1993). This conversion assumes that in response to hyposmolality the initial transient decrease in light scattering is a consequence of osmometric swelling and compensatory RVD. To quantify each of them, the composite light scattering behavior was first deconvoluted by performing a four-parameter fit of the experimental data ($z(t)$) to an Exponential Associate function (EAf) with ORIGIN™ software (Microcal, Northampton, MA 01060). The function was:

$$z(t) = 1 + A\,[1 - exp(-t/\tau_{osm})] + R\,[1 - exp(-t/\tau_{vr})] \quad (1)$$

where:

$$z = \frac{V - b}{V_o - b},$$

$z$ is the relative cell volume; $V$ and $V_O$ are the time-transient and initial cell volumes; $b$ is the cell osmotic inactive volume; $\tau_{osm}$ and $\tau_{vr}$ are the characteristic times of the osmotic and regulatory volume responses, respectively; $R$ is the amplitude of the regulatory volume response to such challenge; and $A$ is the amplitude of a given volume response to anisosmotic challenge. The parameters $A$, $R$, $\tau_{osm}$ and $\tau_{vr}$ were optimized by minimizing $\chi 2$. A further correction to the relative cell volume is necessary if the maximum relative cell volume increase recorded during a transient is not equal to the theoretical value expected for an ideal osmometer. In our case, the initial osmotic transient includes both osmometric swelling as well as the onset of RVD as exemplified in Fig. 1, so this correction is warranted. Using Eq. 1, the time transient volume response is deconvoluted into the sum of two exponential responses. In this fashion, the osmometric and regulatory volume responses are separated, and the fit parameter A (amplitude of osmotic response) can be used for normalization by equating $A$ to the volume change $(A = C_O - C_f)/C_f)$, where $C_O$ and $C_f$ are the initial and final osmolarities, and $(C_O - C_f)/C_f)$ is the normalized volume change for an ideal osmometer. The normalized volume $Zn(t)$ is therefore:

$$z_n(t) = 1 + [z(t) - z(o)] \cdot \frac{C_o - C_f}{A \cdot C_f} \quad (2)$$

The extent of recovery (%) after RVD is defined as $R/A \cdot 100$, and the intensity of the RVD response is characterized by $\tau_{osm}$ and $\tau_{vr}$. As shown in Fig. 1, the data is well described by the function. Data are expressed as means ± SE. Analyses were performed using Student's two-way $t$ test for independent means on paired data.

*Experimental Media.* The control medium was (in mM): NaCl 150; $K_2HPO_4$ 1.6; $KH_2PO_4$ 0.4; $CaCl_2$ 0.7; $MgCl_2$ 1; glucose 5. A 25% hypotonic solution was achieved by decreasing the [NaCl] on an osmolar basis. $CaCl_2$ was omitted from Ca-free NaCl medium, which contained instead 0.5 mM EGTA.

*Materials.* Cyclopiazonic acid (CPA) was purchased from Research Biochemicals International (Natick, MA). Ryanodine was obtained from Calbiochem Corp (La Jolla, CA). EGF and insulin were purchased from Upstate Biotechnology (Lake Placid, NY). All other chemicals were of analytical grade and supplied by Sigma (St. Louis, MO).

## Results

### Separation of the Dependence of Regulatory Volume Response on Extracellular and Intracellular $Ca^{2+}$

To be able to perform paired experiments using the same coverslip, we first investigated whether control RVD responses to two consecutive hypotonic exposures differed from one another. In six different coverslips (*data not shown*), the successive responses were indistinguishable, so each coverslip could serve as its own control. Figure 1 is a composite which shows the average light scattering responses to a 25% hypotonic $Ca^{2+}$-containing medium under four different experimental conditions. In each panel (*A–D*), the control responses are shown together with the test responses. In each case, a control response was followed by 15-min period during which cells were allowed to recover in isotonic medium (*not shown*). During the last 3 min of this recovery period, the cells were preincubated under the particular test condition before being challenged again with a 25% hypotonic stress. Each test condition was maintained during the entire hypotonic exposure.

Figure 1*A* shows the paired responses to hypotonic stress in the presence and nominal absence of ambient $Ca^{2+}$. In the presence of $Ca^{2+}$, there is a rapid initial increase of the relative cell volume to a level lower than expected for osmometric swelling (1.33); we presume

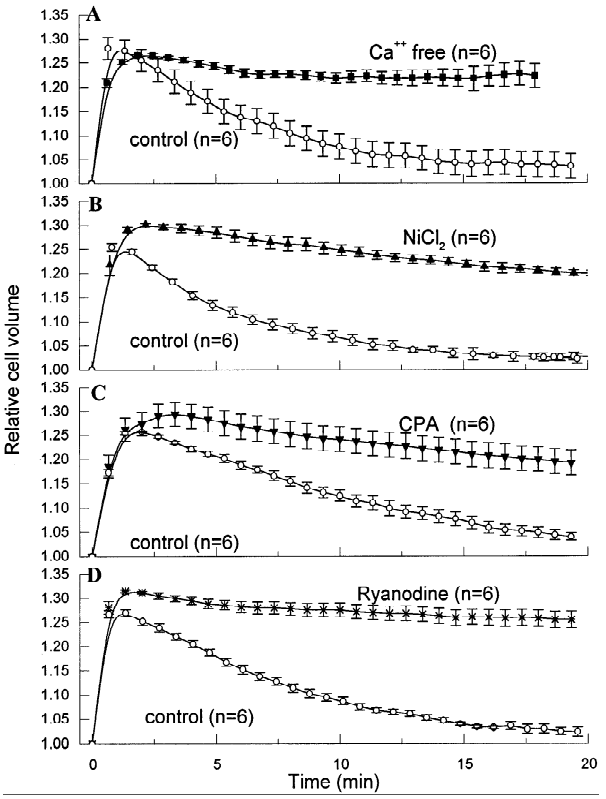


**Fig. 1.** Inhibition of RVD responses to hypotonic stress in tRCE cells. Cells were initially exposed to isotonic $Ca^{2+}$-containing medium (300 mOsm) prior to start of trace. In each panel, the results are shown as the means ± SEM of six paired experiments. Panel (*A*) Effect of $Ca^{2+}$-free medium. The control response to the hypotonic challenge is shown with open circles. The response during exposure to $Ca^{2+}$-free medium is indicated by filled squares. Panel (*B*) Effect of 5 mM $Ni^{2+}$ in $Ca^{2+}$-containing medium: The control response to the hypotonic challenge is shown with open circles. The response during exposure to $Ni^{2+}$ is indicated by filled triangles. (*C*) Effect of 10 μM cyclopiazonic acid (CPA): The control response to the hypotonic challenge is shown with open circles. The response during exposure to CPA is indicated by filled inverted triangles. (*D*) Effect of 100 μM ryanodine: The control response to the hypotonic challenge is shown with open circles. The response during exposure to ryanodine is indicated by crosses.

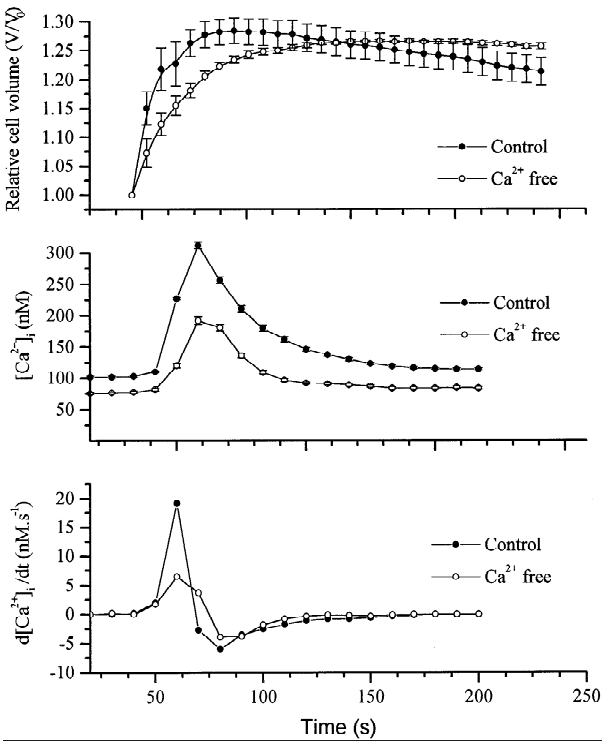


**Fig. 2.** Relationship between time-dependent changes in relative cell volume and $[Ca^{2+}]_i$ Upper panel shows a portion of the light scattering behavior replotted from Fig. 1 *A* on an expanded time scale. The portion is the effect seen immediately following hypotonic stress. Middle panel provides the parallel changes in $[Ca^{2+}]_i$ in the presence ($n = 20$ cells) and nominal absence of extracellular $Ca^{2+}$ ($n = 18$ cells). Values are means ± SEM. Bottom panel shows the calculated slopes of the measured $[Ca^{2+}]_i$ transients depicted in the middle panel.

this is due to an early onset of RVD, while the osmometric response is still taking place. The subsequent volume decline is due to RVD. In the absence of $Ca^{2+}$, the initial rate of swelling is somewhat slower, and RVD is nearly abolished. In quantitative terms, in the presence of $Ca^{2+}$ ($n = 6$), the extent of recovery was 93 ± 4% and the characteristic time ($\tau_{vr}$) was 5.8 ± 0.1 min. In the absence of $Ca^{2+}$, recovery fell to 33 ± 3% ($P < 0.001$). Paradoxically, even though recovery was markedly inhibited, $\tau_{vr}$ also decreased; it fell by 52% to 2.8 ± 0.2 min ($P < 0.05$). Hence, RVD is dependent on the presence of extracellular $Ca^{2+}$.

The $[Ca^{2+}]_i$ profile measurements were done using a protocol similar to that utilized for light scattering, since consecutive exposures to the same hypotonic stress under control conditions elicited $[Ca^{2+}]_i$ transients that were indistinguishable from one another (*data not shown*). To determine if there is a relationship between the inhibition of RVD by $Ca^{2+}$ removal and the $[Ca^{2+}]_i$ response to hypotonicity, the initial effects on relative cell volume and $[Ca^{2+}]_i$ profile are shown together in Fig. 2. The volume transient data of Fig. 1 *A* are shown in an expanded time scale in Fig. 2 (top panel) for comparison with the effects of hypotonicity on the $[Ca^{2+}]_i$ profile (middle panel). To be noted, a temporal comparison between these two measurements is meaningful because the characteristic times during solution exchanges in the two systems are nearly identical to one another.

We investigated the effects of hypotonic challenge with a $Ca^{2+}$-containing medium on $[Ca^{2+}]_i$ in 20 individual cells from six coverslips. The average data and SEMs are shown in Fig. 2 (middle panel). The $[Ca^{2+}]_i$ transient was biphasic. Following hypotonic challenge, $[Ca^{2+}]_i$ rose in about 20 sec from 100 ± 7 nM to a peak of 316 ± 6 nM ($P < 0.001$). Subsequently, $[Ca^{2+}]_i$ decreased gradually to 114 ± 7 nM after 100 sec, which

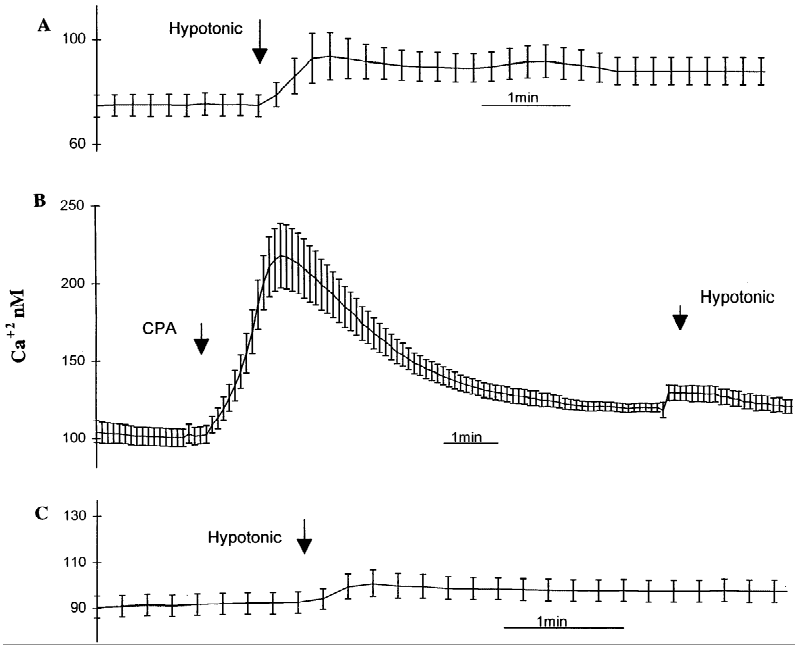


**Fig. 3.** Effects of inhibition of plasmalemma $Ca^{2+}$ influx and intracellular store (ICS) $Ca^{2+}$ release on hypotonic induced $[Ca^{2+}]_i$ transient. With $Ni^{2+}$ (panel *A*) and ryanodine (panel *C*), they were present starting 3 min before substitution of isosmotic $Ca^{2+}$-containing medium and also in the hypotonic (25% dilution) $Ca^{2+}$-containing medium. In panel (*B*), CPA was applied in isotonic medium after stabilization of the $Ca^{2+}$ trace and maintained during the hypotonic challenge. The traces are the average responses ±SEM of the indicated number of cells (*A*) 5 mM $Ni^{2+}$ ($n = 16$ cells). (*B*) 10 μM CPA ($n = 16$ cells) (C) 100 μM ryanodine ($n = 21$ cells).

represents a 94% recovery. In the nominal absence of external $Ca^{2+}$ starting 3 min before hypotonic challenge, $[Ca^{2+}]_i$ rose more slowly, i.e., from 77 ± 8 to 197 ± 26 nM in about 25 sec ($n = 18$ cells). After 75 sec, $[Ca^{2+}]_i$ fell to 85 ± 8 nM, representing a 93% recovery.

The rates of $[Ca^{2+}]_i$ change in the presence and nominal absence of extracellular $Ca^{2+}$ were determined by calculating the slopes of the $[Ca^{2+}]_i$ transients under both conditions. As shown in the bottom panel of Fig. 2, from the time of onset of the hypotonic stress, in the presence of $Ca^{2+}$, the initial increase occurred with a steeper slope than in the nominal absence of extracellular $Ca^{2+}$. This suggests that the initial increase in $[Ca^{2+}]_i$ appears to include plasmalemma $Ca^{2+}$ influx, but during this time it is still possible that release of $Ca^{2+}$ from ICS could also be occurring. Thereafter, the rate of decline occurred more rapidly in the presence than in the nominal absence of extracellular $Ca^{2+}$, suggesting that extrusion through plasmalemma and/or ICS $Ca^{2+}$ reaccumulation could occur more rapidly when $[Ca^{2+}]_i$ is elevated above a threshold level that is only reached in the presence of extracellular $Ca^{2+}$.

## Routes of Plasmalemma $Ca^{2+}$ Permeation

There is evidence that there are nonselective cation pathways across the plasmalemma of rabbit corneal epithelial cells that allow permeation of $Ca^{2+}$ and $Mn^{2+}$ and are inhibited by $Ni^{2+}$ (Rich & Rae, 1995). Since these pathways are the only ones identified so far in these cells as a $Ca^{2+}$ entry route, we used the described inhibitory effect of $Ni^{2+}$ to determine if these pathways contribute to $Ca^{2+}$ influx during RVD. Figure 1*B* shows average RVD volume responses in the absence and presence of 5 mM $Ni^{2+}$ (present for 3 min preincubation as well as during hyposmotic challenge). In these paired experiments, the control ($n = 6$) average RVD recovery was 97 ± 3% and the value for $\tau_{vr}$ was 5.0 ± 0.03 min. In the presence of $Ni^{2+}$, RVD recovery was significantly inhibited to 60 ± 2% ($P < 0.001$) and $\tau_{vr}$ increased significantly ($P < 001$) to 18.5 ± 1.3 min. The corresponding effect of hypotonicity on the $[Ca^{2+}]_i$ response in the presence of 5 mM $Ni^{2+}$ is shown in Fig. 3*A* ($n = 16$ cells). The $Ca^{2+}$ transient was markedly blunted with respect to those shown in Fig. 2 (middle). In Fig. 3*A*, $[Ca^{2+}]_i$ increased by only 50% (from 75 ± 4 to 112 ± 9 nM; $P < 0.01$) in 30 sec with practically no recovery. This agreement between the inhibitory effects of $Ni^{2+}$ on RVD and on the transient $[Ca^{2+}]_i$ response indicates that $Ni^{2+}$-sensitive pathway(s) provide a route for $Ca^{2+}$ influx during RVD.

## Requirement of CICR for Regulatory Volume Decrease

We took a second approach to investigate whether the RVD response required mobilization of $Ca^{2+}$ from ICS. According to the CICR model, the initial emptying of ICS $Ca^{2+}$ results from the stimulation of $Ca^{2+}$ release via $IP_3$-sensitive and/or ryanodine-sensitive channels in the ICS. It is known that ICS emptying elicits an increase in plasmalemma $Ca^{2+}$ influx through an unknown feedback signal. Therefore, to test for CICR involvement, we preceded hyposmotic challenge by either: (i) depleting ICS $Ca^{2+}$ content or (ii) inhibiting release of ICS $Ca^{2+}$

through ryanodine-sensitive channels. In the first case, $Ca^{2+}$ accumulation by the ICS was interfered with by inhibiting the endoplasmic reticulum ATP-dependent $Ca^{2+}$ pump with 10 μM cyclopiazonic acid (CPA) (Seidler et al., 1989).

*Volume Response*

The average volume response ($n = 6$) to hypotonicity in the presence of CPA shown in Fig. 1*C* indicates that depleting ICS of $Ca^{2+}$ caused the recovery to fall from 97 ± 4% to 57 ± 3% ($P < 0.001$) and $\tau_{vr}$ to increase from 8.8 ± 0.2 to 14 ± 0.7 min ($P < 0.02$).

*$Ca^{2+}$ Response*

The corresponding effects of CPA on $[Ca^{2+}]_i$ in the presence of extracellular $Ca^{2+}$ are exemplified in Fig. 3*B*. On the average ($n = 16$ cells), addition of 10 μM CPA caused a biphasic response: initially $[Ca^{2+}]_i$ increased from 90 ± 9 to 185 ± 18 nM in 100 sec ($P < 0.001$), and then gradually fell to a stable value of 120 ± 5 nM ($P < 0.05$ relative to control and peak values) after 330 sec, representing a 68% recovery. Subsequent exposure to hypotonicity (while maintaining exposure to CPA) had no significant effect ($P > 0.05$) on $[Ca^{2+}]_i$; this strongly suggests that the $[Ca^{2+}]_i$ transient response to hypotonicity depends on the amount of $Ca^{2+}$ in the ICS, which has been referred to as its filling state (Jacob, 1990).

For the second case, we investigated the characteristics of RVD and $[Ca^{2+}]_i$ transients after exposure to 100 μM ryanodine. At this concentration, ryanodine is an effective and selective inhibitor of $Ca^{2+}$ release (Meissner, 1996). Figure 1*D* shows average RVD responses ($n = 6$) before and after exposure to 100 μM ryanodine. This inhibitor caused the extent of recovery to significantly fall ($P < 0.001$) from 100 ± 3% to 32 ± 2% whereas $\tau_{vr}$ significantly increased ($P < 0.01$) from 8.0 to 0.1 to 9.7 ± 0.1 min. The corresponding effects of 100 μM ryanodine on hyposmotically-induced $[Ca^{2+}]_i$ transient changes shown in Fig. 3*C* indicate that 100 μM ryanodine did not affect the $[Ca^{2+}]_i$ baseline level. Subsequent to hyposmotic challenge (in the continued presence of ryanodine), instead of undergoing the characteristic biphasic response shown in the middle panel of Fig. 2, $[Ca^{2+}]_i$ rose slightly ($P > 0.05$) after about 35 sec from 91 ± 5 nM to a stable value of 101 ± 6 nM ($n = 21$ cells). The parallel inhibitory effects of ryanodine on the hyposmotically induced RVD and $[Ca^{2+}]_i$ transient responses indicate that $Ca^{2+}$ release from ICS via a ryanodine-sensitive pathway is involved in the RVD response.

### Temporal Relationship between $Ca^{2+}$ Filling State of ICS and Hyposmotically Induced Stimulation of $Ca^{2+}$ Influx Across the Plasmalemma

The aforementioned results show that the elevation of $[Ca^{2+}]_i$ associated with RVD is dependent on both the presence of extracellular $Ca^{2+}$ and the release of $Ca^{2+}$ from ICS. Hence, the mechanism for the elevation of $[Ca^{2+}]_i$ is consistent with CICR. If so, the influx of $Ca^{2+}$ across the plasmalemma would be inversely related to the ICS $Ca^{2+}$ content or its filling state. We therefore varied the ICS $Ca^{2+}$ filling state and determined plasmalemma $Ca^{2+}$ influx by measuring the $Mn^{2+}$ quenching of fura-2 fluorescence (Hallam et al., 1989; Jacob, 1990). The amount of $Ca_i^{2+}$ available for release from the ICS was varied by either depleting the $Ca^{2+}$ stores via treatment with 10 μM CPA in a nominally $Ca^{2+}$-free medium, or by selectively inhibiting $Ca^{2+}$ release with 100 μM ryanodine (Meissner, 1986). Following either of these procedures, the effect of hyposmotic exposure on $Mn^{2+}$ influx was calculated. This calculation took into account decreases in fura 2-fluorescence caused by bleaching and the physical maneuver of solution substitution. This was done by subtracting their rates of decline from all other measurements. (*a*) Depletion experiments. Figure 4 shows the accumulation of intracellular $Mn^{2+}$ as a function of time. Based on the extent of quench under five different conditions, values for $Mn^{2+}$ permeability were calculated as described below: 1. sham isotonic; 2. 25% dilution; 3. 25% dilution with 10 μM CPA; 4. 25% dilution with 100 μM ryanodine and 5. 25% dilution with 10 μM CPA and 100 μM ryanodine. The $Mn^{2+}$ influx under isotonic conditions is representative merely of background dye bleaching. As can be seen, the calculated $Mn^{2+}$ influx subsequent to hypotonic exposure was unchanged with respect to background influx if ICS $Ca^{2+}$ release was blocked with 100 μM ryanodine. The influx was also unchanged with respect to background if 10 μM CPA was present along with 100 μM ryanodine. (*b*) Magnitude of the $Ca^{2+}$ influx through the plasmalemma. To validate the putative involvement of CICR in RVD, The $Mn^{2+}$ quench data were used to calculate plasmalemma $Mn^{2+}$ influx and permeability as an index of $Ca^{2+}$ influx and permeability. For each condition listed above, the time course of the $Mn^{2+}$ influx data were fitted using Origin™ software to a function which included two terms, one describing the exponential buildup of $Mn^{2+}$ following hypotonic challenge, and the second one the baseline influx of $Mn^{2+}$ (linear term):

$$C = Cf \times (1 - e^{-kxt}) + B \times t, \quad (3)$$

where $C$ is the $[Mn^{2+}]$, $C_f$ is the steady state $[Mn^{2+}]$ attributable to entry through nonselective nonvoltage-dependent ionic channels after hypotonic challenge, $k$ is the rate constant, and $B$ is the slope of a quasilinear component of $Mn^{2+}$ entry into quiescent cells continuing also after stimulation. From this expression, after hypotonic challenge the instantaneous rate of change $dC/dt$ of the intracellular $[Mn^{2+}]$ attributable to entry through pathways stimulated by $Ca^{2+}$ release from ICS:

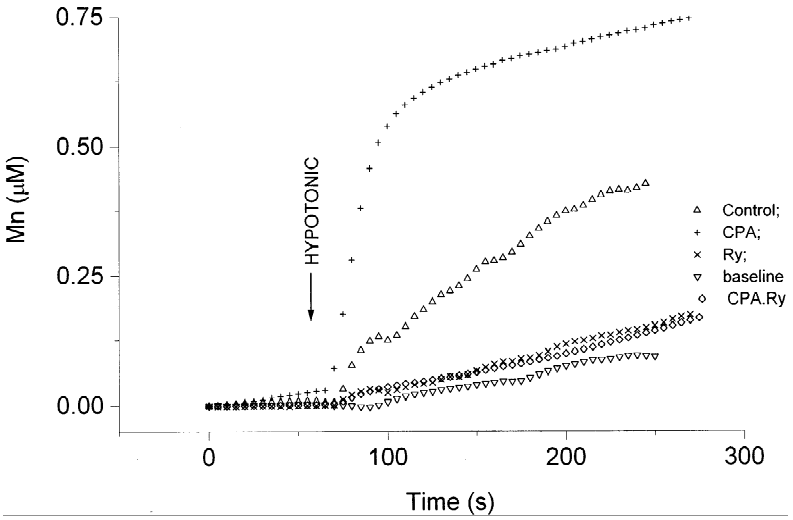


**Fig. 4.** Hypotonic induced accumulation of $Mn^{2+}$ by tRCE as a function of ICS $Ca^{2+}$ filling state. From the indicated time, (*see* arrow) cells are continuously exposed to 0.5 mM $Mn^{2+}$. In four out of the five conditions, $Mn^{2+}$ exposure occurred in a 25% hypotonic nominally $Ca^{2+}$-free medium. The one exception is where $Mn^{2+}$ exposure occurred in isotonic nominally $Ca^{2+}$-free medium. Ryanodine was present at 100 μM whereas CPA was present at 10 μM. Each symbol is the mean of from 4–7 cells per 5–8 coverslips. The indicated error bar is representative of the SEM. *See* insert for definition of symbols.

$$\frac{dC}{dt_{(t=0)}} = k \times C + B \tag{4}$$

Assuming nearly cylindrical shape for the cells, their volume/tangential area ratio is their height, *h*. Hence, the $Mn^{2+}$ influx *J* will be:

$$J = \frac{dC}{dt_{(t=0)}} \times h;$$

the current density *I* corresponding to the $Mn^{2+}$ influx is: $I = z \times F \times J$, where $z = 2$ equivs/mol and *F* is Faraday's constant. Using the Goldman-Hodgkin-Katz formulation, and putting $\xi = zFE/RT$, where *E* is the intracellular potential, *R* the gas constant and *T* the absolute temperature, the plasmalemma permeability *P* for $Mn^{2+}$ is:

$$P = J \times \frac{R \times T}{z \times F \times E} \times \frac{(1 - e^{\xi})}{(M)_e - (M)_1 \times e^{\xi}} \tag{5}$$

$(M)_e$ and $(M)_i$ represent the extracellular and intracellular $Mn^{2+}$ concentrations, respectively. For our calculations, we used values of $h = 15$ μm, $E = -70$ mV, $T = 310$ *K*, and $(M)_e = 500$ μM. $(M)_e$ was assumed to equal zero.

The effects of hypotonic exposure on $Mn^{2+}$ influx shown in Fig. 4 are consistent with CICR involvement in the RVD response. Depleting the ICS $Ca^{2+}$ content prior to hypotonic exposure caused the plasmalemma $Mn^{2+}$ permeability to increase about 6-fold, from $6.9 \times 10^{-8}$ cm/sec (upward triangles in Fig. 4) to $3.8 \times 10^{-7}$ cm/sec (crosses in Fig. 4). Furthermore, the presumed mode of action of 100 μM ryanodine as an inhibitor of ICS $Ca^{2+}$ depletion is validated with this approach. At this concentration of ryanodine, the $Mn^{2+}$ permeability was the same as in the presence of either CPA alone or when CPA and ryanodine were combined with one another. The invariance of the $Mn^{2+}$ permeability is consistent with the assumption that 100 μM ryanodine inhibits ryanodine-sensitive ICS $Ca^{2+}$ release. On the other hand, if ryanodine had instead stimulated release, the $Mn^{2+}$ permeability ought to have been larger than in the presence of CPA.

## Discussion

Our evidence suggests that: (i) CICR is a component of the $Ca^{2+}$ signaling mechanism responsible for eliciting RVD in response to hypotonic challenge; and (ii) for CICR to trigger RVD, $Ca^{2+}$ release from ICS must occur through ryanodine-sensitive channels. In two earlier reports, CICR and $Ca^{2+}$ release from ICS through ryanodine-sensitive channels were reported to be involved in the RVD response. However, in each case the results were not definitive because they did not clearly demonstrate that ryanodine sensitive $Ca^{2+}$ release is a prerequisite for triggering plasmalemma $Ca^{2+}$ influx and RVD. In work done with an intestinal epithelial cell line (Hazama & Okada, 1990), even though ryanodine was used, the contributions of ICS $Ca^{2+}$ release and plasmalemma $Ca^{2+}$ influx to the $[Ca^{2+}]_i$ transient measured in $Ca^{2+}$-containing medium, which are associated with RVD, were not resolved. In another report (work done with medullary collecting duct cells; Tinel et al., 1994), ryanodine was not used; the inhibitors which were used were presumed to inhibit ICS $Ca^{2+}$ release, but their mode of action was not verified, so it remained possible that other mechanisms were also involved in triggering RVD in this preparation. In contradistinction, we show here unequivocally that ryanodine-sensitive $Ca^{2+}$ release from intracellular stores along with CICR are requirements for regulatory volume decrease in transformed rabbit corneal epithelial cells.

In response to a hypotonic stress, many cells can restore their initial volume through RVD. This response involves intracellular water loss subsequent to osmolyte efflux. One mechanism for osmolyte efflux can include stimulation of specific membrane ion transport pathways. For example in red cells, the osmotic response to a dilution of the bathing solution includes an increase in KCl efflux (Cala, 1983). There is also some suggestive evidence that a response involving increased $Cl^-$ efflux may occur in the corneal epithelium because elevations of $[Ca^{2+}]_i$ stimulate transepithelial net $Cl^-$ transport (Candia, Montoreano & Podos, 1977). A stimulatory effect on $Cl^-$ efflux can also be elicited by different adrenergic agonists and direct stimulation of adenylate cyclase with forskolin; they all cause transient elevations in $[Ca^{2+}]_i$, cAMP accumulation and stimulation of cAMP sensitive basolateral $K^+$ and apical membrane $Cl^-$ permeabilities (Nagel & Reinach, 1980; Wolosin & Candia, 1987; Reinach et al., 1992). As we show here that RVD elicits elevations in $[Ca^{2+}]_i$, from the prior evidence cited, an increase in KCl efflux could form part of this volume regulatory response in these cells.

Exposure to $Ni^{2+}$ or the removal of $Ca^{2+}$ from the medium inhibited both RVD and the $[Ca^{2+}]_i$ transient seen under control conditions (Fig. 2 middle panel). Even though $Ni^{2+}$ inhibited the $[Ca^{2+}]_i$ transient more than did $Ca^{2+}$ removal, $Ca^{2+}$ removal had a larger inhibitory effect on RVD than $Ni^{2+}$. This dissociation between the extent of inhibition of the $[Ca^{2+}]_i$ transient and RVD suggests that each of these procedures affects other phenomena in addition to plasmalemma influx. It is conceivable that $Ni^{2+}$ like $Mn^{2+}$ permeates into the cell interior. In addition to quenching fura2, in the cerebellum, $Mn^{2+}$ can inhibit ICS function (Striggow & Ehrlich, 1996). $Ni^{2+}$ may have a similar effect whereas $Ca^{2+}$ removal is restricted to inhibiting plasmalemma $Ca^{2+}$ influx and filling of ICS $Ca^{2+}$ content. On the other hand, the larger inhibitory effect of $Ca^{2+}$ removal on RVD could indicate that EGTA and/or $Ca^{2+}$ removal have other nonspecific membrane effects one of which may be a decrease in ion permeability. One possible indication of such an effect is that the rate of osmotic swelling shown in Fig. 1*A* ($Ca^{2+}$-free) was slower than in Fig. 1*B* ($Ni^{2+}$).

Another indication that $Ni^{2+}$ may also inhibit an ICS function is based on a comparison of its effects to those of CPA. In the presence of $Ca^{2+}$ in the medium, the inhibitory effects of $Ni^{2+}$ and CPA on RVD and $[Ca^{2+}]_i$ transients were similar to one another (Figs. 1 and 3). CPA and $Ni^{2+}$ inhibited RVD recovery by 40% and 37%, respectively, and the values for $\tau_{vr}$ were lengthened by 68% and 270%, respectively. In both cases, hypotonicity failed to elicit a $[Ca^{2+}]_i$ transient which even resembled the response obtained under control conditions (Fig. 2 middle panel). Finally, the inhibitory effect of $Ni^{2+}$ on the hypotonicity-induced $[Ca^{2+}]_i$ transient was similar to that of 100 $\mu$M ryanodine (Fig. 3*C*) further indicating that $Ni^{2+}$ may affect an ICS function.

The concept of CICR has evolved based on observations that in a variety of cell types there is an increase in plasmalemma permeability to divalent cations subsequent to $IP_3$ receptor stimulation which mediates $Ca^{2+}$ release from ICS (Ambudkar et al., 1993; Muallem, Khademazad & Sachs, 1990; Putney & Bird, 1993). This increase in plasmalemma permeability is directly related with the depletion state of the ICS, since repletion of the ICS $Ca^{2+}$ content results in a decrease of $Ca^{2+}$ influx (Ambudkar et al., 1993; Muallem et al., 1990; Putney & Bird, 1993). The feedback mechanism responsible for regulating plasmalemma $Ca^{2+}$ influx is not known. In order to determine whether CICR is involved in a response, it is necessary to show that: (i) the inhibition of $Ca^{2+}$ release from ICS inhibits the response in question; (ii) changes in plasmalemma $Ca^{2+}$ influx are a consequence of an alteration in the availability of $Ca^{2+}$ for release from its ICS.

The transient increase in $[Ca^{2+}]_i$ resulting from exposure to CPA in $Ca^{2+}$ containing medium is consistent with a relationship between ICS $Ca^{2+}$ content and plasmalemma $Ca^{2+}$ influx. Subsequent to the inhibition of the ICS $Ca^{2+}$ pump activity ICS $Ca^{2+}$ content decreased as a result of the loss of $Ca^{2+}$ through $IP_3$ and ryanodine sensitive channels. Accordingly, $[Ca^{2+}]_i$ may have risen for two reasons: (i) blockage of ICS $Ca^{2+}$ accumulation by CPA; (ii) increase in plasmalemma $Ca^{2+}$ influx owing to a depletion of ICS $Ca^{2+}$ content. The subsequent decline of the transient is presumably due to the stimulation of plasma membrane $Na^+/Ca^{2+}$ exchange and ATP dependent $Ca^{2+}$ pump activity (Rich & Rae, 1995; Reinach & Holmberg, 1991).

From our current evidence, it is apparent that both plasmalemma $Ca^{2+}$ influx and $Ca^{2+}$ release from ICS were required for RVD to occur. The inhibitory effects of either the nominal absence of $Ca^{2+}$ in the medium or 5 mM $Ni^{2+}$ on RVD and the $[Ca^{2+}]_i$ transient (Figs. 1 and 3) strongly suggest a role for plasmalemma $Ca^{2+}$ influx. However, plasmalemma $Ca^{2+}$ influx is not sufficient to trigger RVD. In the presence of $Ca^{2+}$ in the medium and following depletion of ICS $Ca^{2+}$ content by exposure to 10 $\mu$M CPA, hypotonicity failed to increase the $[Ca^{2+}]_i$ (Fig. 3) and the RVD response was significantly inhibited (Fig. 1). In addition, exposure to 10 $\mu$M U73122 (a known inhibitor of $IP_3$ formation) did not block the RVD response (*data not shown*). These results show that both plasmalemma $Ca^{2+}$ influx and ICS $Ca^{2+}$ release are involved in the RVD response. However, any temporal interdependence between these mechanisms could not be ascertained based on the effects of $Ni^{2+}$ and CPA, which is why we investigated whether there is a relationship

between the ICS $Ca^{2+}$ filling state and plasmalemma $Mn^{2+}$ influx, as discussed below.

$Mn^{2+}$ quenching of fura2-fluorescence determined in a nominally $Ca^{2+}$ free medium has been taken only as a relative measure of plasmalemma $Ca^{2+}$ permeability, since it is unclear whether only plasmalemma $Ca^{2+}$ channels are permeant to $Mn^{2+}$ (Jacob, 1990). As another relevant limitation, it was shown recently that in the cerebellum, $Mn^{2+}$ quenching may reflect its permeation through a $IP_3$ receptor/$Ca^{2+}$ channel into ICS (Striggow & Ehrlich, 1996). If these last results are applicable to corneal epithelial cells, the interpretation of the $Mn^{2+}$ quench experiments may be dubious. With these caveats, the $Mn^{2+}$ influx following hypotonic exposure was affected by the $Ca^{2+}$ filling state of the ICS. After depletion of the ICS $Ca^{2+}$ content with 10 $\mu$M CPA, the calculated permeability to $Mn^{2+}$ was about 6-fold larger than in the absence of CPA. On the other hand, if $Ca^{2+}$ release through the ryanodine sensitive pathways was blocked, the $Mn^{2+}$ permeability following hypotonic exposure was the same as that calculated during a sham isotonic substitution. It has been reported that comparatively low [ryanodine] can stimulate (rather than inhibit) $Ca^{2+}$ release from ICS (Meissner, 1986). However, evidence that the [ryanodine] employed here was appropriate to inhibit $Ca^{2+}$ release comes from the fact that 100 $\mu$M ryanodine decreased markedly the effect of hypotonicity on $Mn^{2+}$ influx in cells exposed to CPA. Had ryanodine stimulated $Ca^{2+}$ release, we would have observed instead an increase in $Mn^{2+}$ influx, a we do when CPA alone is utilized (Fig. 4). Taken together, our evidence strongly suggests that $Ca^{2+}$ release through a ryanodine-sensitive channel along with $Ca^{2+}$ influx through the plasmalemma are both necessary to mediate RVD.

This work was supported by National Institutes of Health grants EY 06718 (JF) and EY 04795 (PR) and the RPB, Inc. The support from Santen Pharmaceutical is also deeply appreciated. We are especially indebted to Dr. Araki Sasaki, Kinki University, Hyogo, Japan for her generous provision of SV40-virus transformed rabbit corneal epithelial cells.

## References

Ambudkar, I.S., Hiramatsu, Y., Lockwich, T., Baum, B.J. 1993. Activation and regulation of calcium entry in rat parotid gland acinar cells. *Crit. Rev. Oral Biol. Med.* **4:**421–425

Araki-Sasaki, A., Ohashi, Y., Sasabe, T. 1993. Immortalization of rabbit corneal epithelial cells by a recombinant SV40-adenovirus vector. *Invest. Ophthal. Vis. Sci.* **34:**2665–2671

Bencherif, M., Eisenhour, C.M., Prince, R.J., Lippiello, P.M., Lukas, R.J. 1995. The ''calcium antagonist'' TMB-8 [3,4,5-trimethoxybenzoic acid 8-(diethylamino)octyl ester] is a potent, noncompetitive, functional antagonist at diverse nicotinic acetylcholine receptor subtypes. *J. Pharmacol. Exp. Ther.* **275:**1418–1426

Cala, P.M. 1983. Volume regulation by red blood cells Mechanisms of ion transport. *Mol. Physiol.* **4:**33–47

Candia, O.A. 1976. Fluid and chloride transport by the epithelium of the isolated frog cornea. *Fed. Proc.* (part 1) 703

Candia, O.A., Montoreano, R., Podos, S.M. 1977. Effect of the ionophore A23187 on chloride transport across isolated frog cornea. *Am. J. Physiol.* **233(2):**F94–F101

Candia, O.A., Zamudio, A. 1995. Chloride activated water permeability in the frog corneal epithelium. *J. Membrane Biol.* **143:**259–266

Chamberlin, M.E., Strange, K. 1989. Anismotic cell volume regulation: a comparative view. *Am. J. Physiol.* **257:**C159–173

Dassouli, A., Sulpice, J.C., Roux, S., Crozatier, B. 1993. Stretch-induced inositol triphosphate and tetrakisphosphate production in rat cardiomyocytes. *J. Molecular and Cellular Cardiology* **25:**973–982

Fischbarg, J., Lim, J.J., Bourguet, J. 1977. Adenosine stimulation of fluid transport across rabbit corneal endothelium. *J. Membrane Biol.* **35:**95–112

Fischbarg, J., Li, J., Kuang, K., Echevarria, M., Iserovich, P. 1993. Determination of volume and water permeability of plated cells from measurements of light scattering. *Am. J. Physiol.* **265:**C1412–C1423

Foskett, K. 1994. The role of calcium in the control of volume-regulatory transport pathways. *In:* Cellular and Molecular Physiology of Cell Volume Regulation. K. Strange, editor. pp. 259–277. CRC Press

Hallam, T.J., Jacob, R., Merritt, J.E. 1989. Influx of bivalent cations can be independent of receptor stimulation in endothelial cells. *Biochem. J.* **259:**125–129

Hazama, A., Okada, Y. 1990. Involvement of $Ca^{2+}$-induced $Ca^{2+}$ release in the volume regulation of human epithelial cells exposed to a hypotonic medium. *Biochem. Biophys. Res. Commun.* **17:**287–293

Ishii, T., Hashimoto, T., Ohmori, H. 1996. Hypotonic stimulation induced $Ca^{2+}$ release from $IP_3$-sensitive internal stores in a green monkey cell line. *J. Physiol.* **493:**371–383

Islam, M.S., Larsson, O., Nilsson, T., Berggren, P.O. 1995. Effects of caffeine on cytoplasmic free $Ca^{2+}$ concentration in pancreatic beta cells are mediated by interaction with ATP-sensitive $K^+$ channels and L-type voltage-gated $Ca^{2+}$ channels but not the ryanodine receptor. *Biochem. J.* **306:**679–686

Jacob, R. 1990. Agonist-stimulated divalent cation entry into single cultured human umbilical vein endothelial cells. *J. Physiol.* **421:**55–77

Klyce, S.D. 1977. Enhancing fluid secretion by the corneal epithelium. *Invest. Ophthal. Vis. Sci.* **16:**968–973

Klyce, S.D., Beuerman, R.W. 1988. Structure and function of cornea. *In:* The Cornea. H.E. Kaufman, B.A., Barron, M. Mcdonald, editors. Churchill Livingstone

Margalit, A., Livine, A.A., Funder, J., Granot, Y. 1993. Initiation of RVD response in human platelets mechanical-biochemical transduction involves pertussin-toxin sensitive G protein and phospholipase $A_2$. *J. Membrane Biol.* **136:**303–311

Maurice, D.M. 1972. The location of the fluid pump in the cornea. *J. Physiol.* 43–54

McCarty, N.A., O'Neil, R.G. 1991*a*. Calcium dependent control of volume regulation in renal proximal tubule cells: *I. Swelling activated $Ca^{2+}$ entry and release. J. Membrane Biol.* **123:**149–160

McCarty, N.A., O'Neil, R.G. 1991*b*. Calcium dependent control of volume regulation in renal proximal tubule cells: Roles of dihydropyridine sensitive and insensitive $Ca^{2+}$ entry pathways. *J. Membrane Biol.* **123:**161–170

Meissner, G. 1986. Ryanodine activation and inhibition of the $Ca^{2+}$

release channel of sarcoplasmic reticulum. *J. Biol.Chem.* **261:**6300–6

Mehkail-Ishak, K., Lavoie, P.A., Sharkawi, M. 1987. Effects of caffeine and cyclic adenosine 3′,5′-monophosphate on adenosine triphosphate-dependent calcium uptake by lysed brain synaptosomes. *Brain Res.* **426:**62–68

Missiaen, L., DeSmedt, H., Parys, J.B., Sienaert, I., Vanlingen, S., Droogmans, G., Nilius, B., Casteels, R. 1996. Hypotonically induced calcium release from intracellular calcium stores. *J. Biol. Chem.* **271:**4601–4604

Muallem, S., Khademazad, M., Sachs, G. 1990. Phosphorylation downregulated the store-operated $Ca^{2+}$ entry pathway of human neutrophils. *J. Biol. Chem.* **269:**3963–3967

Nagel, W., Reinach, P. 1980. Mechanism of stimulation by epinephrine of active Cl transport in the isolated frog cornea. *J. Membrane Biol.* **56:**73–79

Putney, J.W. Jr. 1986. A model for receptor-regulated calcium entry. *Cell Calcium* **7:**1–12

Putney, J.W., Bird, G. St. J. 1993. The inositol phosphate calcium signalling system in nonexcitable cells. *Endocr. Rev.* **14:**610–631

Rafizadeh-Montrose, C., Guggino, W. 1991. Role of intracellular calcium in volume regulation by rabbit medullary thick ascending limb cells. *Am. J. Physiol.* **260:**F402–F409

Reinach, P., Holmberg, N. 1989. Inhibition by calcium of beta adrenoceptor mediated cAMP responses in isolated bovine corneal epithelial cells. *Curr. Eye Res.* **8:**85–90

Reinach, P.S., Socci, R.R., Keith, C., Scanlon, M. 1992. Adrenergic receptor mediated increase of intracellular $Ca^{2+}$ concentration in isolated bovine corneal epithelial cells. *Comp. Biochem. Physiol.* **102A:**709–714

Reinach, P.S., Holmberg, N., Chiesa, R. 1991. Identification of calmodulin-sensitive $Ca^{2+}$ transporting ATPase in the plasma membrane of bovine corneal epithelial cells. *Biochim. Biophys. Acta* **1068:**1–8

Rich, A., Rae, J.L. 1995. Calcium entry in rabbit corneal epithelial cells: evidence for a nonvoltage dependent pathway. *J. Membrane Biol.* **144:**177–184

Sakai, T., Ambudkar, I.S. 1996. Role for protein phosphatase in the regulation of $Ca^{2+}$ influx in parotid gland acinar cells. *Am. J. Physiol.* **40:**C284–C294

Seidler, N.W., Jona, I., Vegh, M., Martonosi, A. 1989. Cyclopiazonic acid is a specific inhibitor of the $Ca^{2+}$-ATPase of sarcoplasmic reticulum. *J. Biol. Chem.* **30:**17816–17823

Socci, R.R., Chu, A., Reinach, P., Meszaros, L.G. 1993. In situ $Ca^{2+}$ induced $Ca^{2+}$ release from a ryanodine-sensitive intracellular $Ca^{2+}$ store in corneal epithelial cells. Comp. Biochem. Physiol B **106:**793–797

Striggow, F., Ehrlich, B.E. 1996. The Inositol 1,4,5-triphosphate receptor of cerebellum $Mn^{2+}$ permeability and regulation by cytosolic $Mn^{2+}$. *J. Gen. Physiol.* **108:**115–124

Tinel, H., Wehner, F., Sauer, H. 1994. Intracellular $Ca^{2+}$ release and $Ca^{2+}$ influx during regulatory volume decrease in IMCD cells. *Am. J. Physiol.* **267:**F130–F138

Walz, B., Baumann, O., Zimmerman, B., Ciriacy-Wantrup, E.V. 1995. Caffeine and ryanodine $Ca^{2+}$-induced $Ca^{2+}$ release from the endoplasmic reticulum in honey bee photoreceptors. *J. Gen. Physiol* **105:**537–567

Wolosin, J.M., Candia, O.A. 1987. Cl-secretagogues increase basolateral $K^+$ conductance of frog corneal epithelium. *Am. J. Physiol.* **253:**C555–C560

Wolosin, J.M., Candia, O.A. 1989. Volume regulatory decrease in corneal epithelium. *In:* Membrane Ion Transport and Carriers. J.H. Durham and M. Hardy, editors. *Ann NY Acad. Sci.* **574:**131–133